Optical Feedback Generated by Tapered Amplifiers Emitting at 1120 nm

Nils Werner, Nina Thieß, Katrin Paschke, and Günther Tränkle, *Member, IEEE*

***Abstract*— In this work the optical feedback generated by a tapered amplifier (TPA) emitting at 1120 nm is characterized at different operational conditions. The TPA is operated in a master oscillator power amplifier (MOPA) configuration, while the influence of pump current or seed power on the emitted feedback is investigated. Measurements are also performed with the TPA exposed to defined external optical feedback. For an estimation of the feedback from the TPA a simple formula is derived and the calculations are compared to the measurement results. With the experimental and theoretical results the required feedback resistance of the master oscillator seed source can be defined and the MOPA system optimized for certain applications with unwanted optical feedback.**

***Index Terms*— Optical feedback, semiconductor lasers, tapered amplifier, flared amplifier.**

I. Introduction

SEMICONDUCTOR based high power laser sources emitting around 1120 nm are highly demanded for several applications. As a pump source for nonlinear frequency conversion these lasers enable accessing the yellow-green spectral range. Emission with wavelengths around 561nm is a key for many techniques e.g. in the field of bio-medical sciences [1], [2].

The requirements on such a near infrared emitting pump laser source include watt-level optical output power, high spatial beam quality and narrow spectral bandwidth. Besides single emitter devices like the distributed Bragg-reflector tapered diode laser (DBR-TPL) [3] a hybrid master oscillator power amplifier (MOPA) concept based on a distributed Bragg-reflector ridge waveguide laser (DBR-RWL) and a tapered amplifier (TPA) [4] is well suited for that purpose. In contrast to the simple monolithic DBR-TPL the more complex MOPA setup nevertheless features certain advantages. A hybrid MOPA offers direct modulation capability and a decoupling of the emission wavelength from the optical output power. The separation of the low power master oscillator (MO) from the power amplifier (PA) also allows to shield the MO against possible optical feedback from the TPA by a miniaturized optical isolator. However, the feedback emitted from the TPA towards the DBR-RWL has not been investigated in detail yet.

In addition to the feedback from the TPA the MOPA as a whole can be subject to external feedback as well. For nonlinear frequency conversion the used crystals may have a reflectivity of 1×10^{-4} [5] while typical optical antireflection coatings or bare surfaces like fiber tips may generate even higher feedback up to 1×10^{-2}. The optical feedback to the TPA may deteriorate the spatial beam quality [6], [7] but it can be expected that the backward propagating light is also amplified in the TPA and increases the feedback towards the MO dramatically. With respect to the feedback sensitivity of master oscillators like DBR-RWLs [8] a proper selection of the laser and optical isolator is necessary.

This work addresses the study of the feedback emission characteristics of a TPA emitting at 1120 nm. The feedback power emitted from the TPA is measured for different operating conditions like the electrical pump current and especially under the exposure to defined external feedback. In order to estimate the feedback power from the TPA a simplified formula is derived and the calculations are compared to the measurements. The results allow to either define limits for the maximum acceptable external feedback strength for a given laser system or to optimize and select the best suited components for a certain application.

II. Tapered Amplifier Emitting at 1120 nm

The TPA subject to this study is based on AlGaAs, where the active zone is a double quantum well which is embedded asymmetrically into a 4.8 μm thick waveguide. Further information on the vertical structure and processing steps are found in [9] while the use of such a TPA is presented in [4]. The lateral design of the edge emitting TPA is shown schematically in fig. 1. The device is composed of two sections. An $L_{\mathrm{RW}} = 2\,\mathrm{mm}$ long ridge waveguide (RW) section is formed by etching trenches yielding a $w_{\mathrm{RW}} = 4\,\mu\mathrm{m}$ wide ridge that acts as a mode filter and preamplifier. The RW section is followed by an $L_{\mathrm{TP}} = 4\,\mathrm{mm}$ long tapered (TP) section with a full opening angle of $\theta_{\mathrm{TP}} = 6°$. In the TP section no index guiding takes place, the geometry is only defined by the actively pumped area. Both sections can be electrically pumped individually. In order to suppress self lasing the facets are highly antireflection coated to achieve a residual reflectivity of 1×10^{-4}. Throughout this work the facet near the RW section is considered as the back facet while the facet near the TP section is referred to as the front facet.

Manuscript received September 16, 2021; revised December 21, 2021 and January 18, 2022; accepted January 21, 2022. Date of publication January 26, 2022; date of current version February 11, 2022. *(Corresponding author: Nils Werner.)*

The authors are with the Ferdinand-Braun-Institut gGmbH, Leibniz-Institut für Höchstfrequenztechnik, 12489 Berlin, Germany (e-mail: nils.werner@fbh-berlin.de).

Color versions of one or more figures in this article are available at https://doi.org/10.1109/JQE.2022.3146588.

Digital Object Identifier 10.1109/JQE.2022.3146588

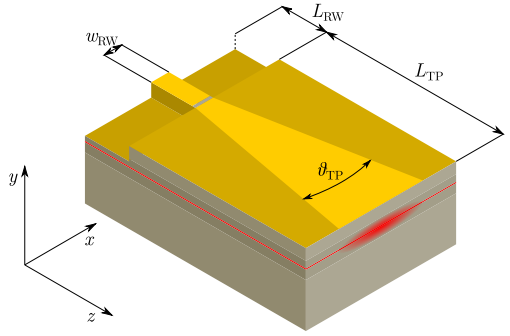

Fig. 1. Schematic of the investigated TPA. The device is separated into an $L_{RW} = 2\,\text{mm}$ long ridge waveguide section and an $L_{TP} = 4\,\text{mm}$ long tapered section. The ridge waveguide has a width $w_{RW} = 4\,\mu\text{m}$ and the tapered section has a full opening angle of $\theta_{TP} = 6°$. The coordinate system indicates the directions used throughout this work.

III. Basic Theoretical Considerations

The optical feedback generated by the TPA in a MOPA configuration may have several origins. Due to the non vanishing facet reflectivities the input beam as well as the amplified output beam are partly reflected. While the reflection from the back facet is straightforward, the reflection at the front facet needs to be considered in more detail. On the one hand the input beam and its reflection is amplified while propagating through the TPA. On the other hand the radiation diverges in the TP section and only a small amount of the reflection is coupled back into the RW section. The remaining light which is not coupled into the RW can reach the back facet and lead to distinct intensity distributions beside the RW [10]–[12]. However, for low facet reflectivities of the order of 1×10^{-3} it has been found that significant intensity of the backward propagating light is only found in the RW [10], while light near the RW is strongly attenuated.

A second origin of optical feedback arises from external reflections of the amplified output power. In most practical cases the emission from the TPA is collimated and then may pass a system of optical elements. At reflecting interfaces the beam is then often reflected into itself, directly entering the TPA and being amplified as well. In contrast to the reflection of the back facet, the radiation converges in the TP section and is coupled into the RW to a high degree. Therefore, the external feedback may have a strong impact on the feedback emitted from the TPA. It has to be stated that feedback originating from scenarios other than the previously described with the output beam not being ideally reflected into itself different effects can occur. While misalignment in the lateral (x-direction) cause light propagating outside the RW and reach the back facet, it is also possible that higher order vertical modes are excited in case of vertical misalignment [13].

In addition to the feedback caused by reflections of the laser radiation the TPA also emits amplified spontaneous emission (ASE) [14].

A. Calculation of Feedback Power

In general, the calculation of the feedback power requires an at least 2D simulation of the light propagating through the TPA. Simulations based on a beam propagation method are well suited and may also include ASE emission [15]. But the simulation also requires computational effort and the knowledge of several material parameters of the semiconductor. If only the total feedback power is of interest and light propagation outside the actively pumped areas (e.g. beside the RW) can be neglected, the calculation model can be drastically simplified.

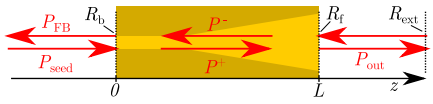

Fig. 2. Schematic of the TPA and quantities used for the theoretical model.

In order to estimate the feedback power emitted from the TPA a simple one-dimensional model based on the power inside the amplifier is used. To be concrete, the forward and backward propagating power inside the amplifier is considered. The TPA is treated as a Fabry-Perot laser [16] with extensions accounting for the input seed and feedback power. A schematic of the TPA and the quantities used in the model are shown in fig. 2.

The forward and backward propagating power along the z-direction inside the TPA obeys the differential equation (1)

$$\frac{\mathrm{d}}{\mathrm{d}z} P^{\pm}(z) = \pm\beta P^{\pm}(z). \tag{1}$$

The constant β includes the gain and loss per unit length and is proportional to the imaginary part of the effective refractive index in the TPA. Equation (1) is subject to the boundary conditions

$$P^{+}(0) = R_b P^{-}(0) + (1 - R_b) P_{\text{seed}} \tag{2}$$

$$P^{-}(L) = \eta R_f P^{+}(L) + (1 - R_f)^2 R_{\text{ext}} P^{+}(L) \tag{3}$$

With the back and front facet lying at $z = 0$ and $z = L$ respectively, where L is the total length of the TPA. The first terms in equations (2) and (3) account for the reflections at the back and front facets with reflectivity R_b and R_f, respectively. The coupling losses of the reflection at the front facet back into the RW section are described by η. Following the geometric beam expansion and calculating the overlap integral the coupling can be estimated [17] to $\eta = 0.0093$. This approach implies that all the light which is not coupled into the RW is properly attenuated and does not reach the back facet. The second terms in equation (2) and (3) model the seed light transmitted through the back facet and the external reflection of the front emitted power with external reflectivity R_{ext}, respectivly. It is assumed here that the external feedback is properly coupled into the vertical waveguide and into the RW after passing the TP section. The contributions of the seed or feedback light and the reflections of the facets in equations (2) and (3) are summed as optical powers. This is equivalent to a resonant superposition of the respective field amplitudes which is a good approximation for vanishing reflectivities R_b and R_f. Reflections of the external feedback at the front facet of the TPA are neglected.

Since the internal power is not directly measurable the forward and backward propagating power $P^{\pm}$ at the facets

are expressed by the feedback power P_{FB} and the output power P_{out}

$$P_{\mathrm{FB}} = P_{\mathrm{seed}} R_b + (1 - R_b) P^-(0) \quad (4)$$

$$P_{\mathrm{out}} = (1 - R_f) P^+(L). \quad (5)$$

The feedback power P_{FB} is the total power that is emitted or reflected from the TPA at $z = 0$ towards the seed source. Here, the first summand in equation (4) results from the reflection of the incident seed light at the back facet. The output power P_{out} is the forward emitted power from the TPA through its front facet at $z = L$ either with or without external feedback.

With equations (2) to (5) a formula for the feedback power can be found. Terms of the form $(1 - R_{b,f})$ are neglected due to the small front and back reflectivities $R_f \ll 1$ and $R_f \ll 1$.

$$P_{\mathrm{FB}} = \left(R_b - \frac{1}{2R_b} \right) P_{\mathrm{seed}} + \sqrt{\frac{P_{\mathrm{seed}}^2}{4R_b^2} + (\eta R_f + R_{\mathrm{ext}}) \frac{P_{\mathrm{out}}^2}{R_b}} \quad (6)$$

Equation (6) only depends on directly accessible quantities like the seed and output power as well as the front, back and external reflectivity. Thus, no knowledge about the internal material properties of the TPA is required making it a universal tool not only suited specifically for the TPA emitting at 1120 nm. However, it has to be mentioned that the model only describes the propagating laser radiation and neglects ASE emission.

In contrast to the feedback caused by reflections of the laser light, the prediction of the ASE feedback is more complicated. Here, the ASE feedback depends on the properties of the semiconductor as well as the propagating optical power. However, the qualitative emission behavior of the ASE in dependency on the internal power can be estimated. With increasing power inside the TPA, e.g. due to higher seed power, the ASE emission is reduced.

IV. Experimental Setup

The experimental setup used for the feedback study of the TPA can be separated into two parts. The first part is a setup to provide the seed power for the TPA and investigate output and feedback emission properties of the TPA in a solitary MOPA configuration. The second part extends the first part to generate controlled optical feedback and measure the emission behavior of the TPA under external feedback conditions.

The experimental setup for the experiments with the solitary MOPA configuration is shown in fig. 3 a). Seed power is provided by a DBR-RWL with a length of 3 mm and a facet reflectivity of 30 % which is described in detail in [8], [18]. The laser emission is collimated by an aspherical lens L1 with a focal length of 8 mm and guided by mirrors through an optical isolator (OI) with an isolation of 40 dB. Then the beam passes the beam splitter BS1 with a reflectivity of 39 % and is coupled into the TPA by an aspherical lens L2 that is similar to the lens L1. With the power detector PD1 the output emission of the TPA is characterized. Possible feedback reflections from the TPA are collimated by lens L2 and guided to a second power detector PD2 or imaged by a camera (CAM). The feedback emission from the TPA is specified by its power

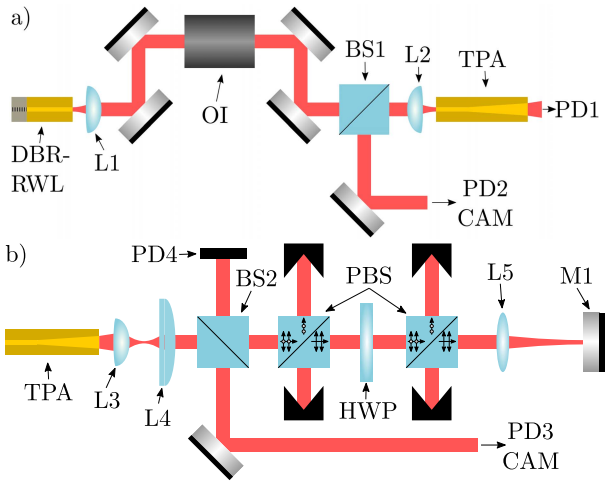

Fig. 3. Schematics of the used experimental setups. a) Setup for the investigation of the output power and feedback emission of the TPA in solitary MOPA configuration. b) Extension of the setup shown in a) to generate defined feedback levels to the TPA.

P_{FB} and also in relation to the seed power P_{seed} as the TPA power feedback ratio $PFR_{\mathrm{TPA}} = 10\,\mathrm{lg}(P_{\mathrm{FB}}/P_{\mathrm{seed}})$. In order to image the back facet onto the camera a spherical lens with a focal length of 400 mm (not shown) is used.

For the experiments with external feedback, the setup is extended behind the TPA. The schematic of the setup is shown in fig. 3 b). Here, the emission from the TPA is collimated vertically, also with an aspherical lens L3 with 8 mm focal length. Due to the astigmatism of the output beam, a second cylindrical lens L4 with 70 mm focal length is required for the collimation in the horizontal direction. With the beam splitter BS2 which has a reflectivity of 44 % a part of the output power is directed to the power detector PD3. Alternatively, the beam waist of the output beam can be imaged onto a camera (CAM) in the same way as the feedback by a spherical lens with 400 mm focal length (not shown). The remaining beam passes two polarizing beam splitters (PBS) and a half wave plate (HWP) that allows for defined attenuation. A combination of a spherical lens L5 with 250 mm focal length and a plane mirror M1, placed near the focal plane of L5, is used to reflect the beam into itself. After passing the PBS and HWP again the power of the feedback can be determined from the reflection at BS2 with the power detector PD4. Thereby the external reflectivity R_{ext} is set which is in the following also defined as the external power feedback ratio $PFR_{\mathrm{ext}} = 10\,\mathrm{lg}(R_{\mathrm{ext}})$. With the setup, power feedback ratios in a range of -60 dB to -20 dB are possible.

In order to ensure a high coupling efficiency of the feedback into the TPA the setup is adjusted accordingly. First, the emission from the TPA is collimated properly for the respective working point, i.e. the RW and TP current. The feedback strength is then set to the highest level of -20 dB and the mirror M1 is adjusted while measuring the feedback power of the TPA. Optimal coupling of the feedback is achieved when the feedback power reaches a maximum.

The setup extension for the external feedback generation is comparable to the setup presented in [8]. As described there

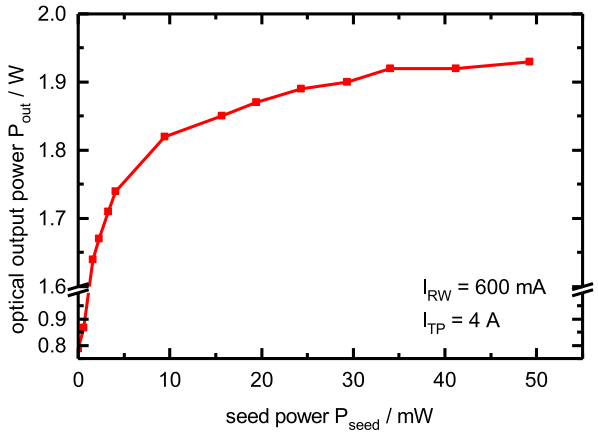

Fig. 4. Output power characteristics of the TPA at a fixed working point with $I_{RW} = 600\,mA$ RW current and $I_{TP} = 4\,A$ TP current as a function of the input seed power.

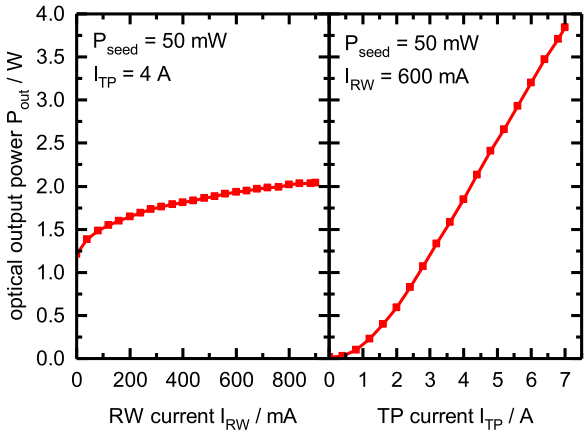

Fig. 5. Output power characteristics of the TPA at a fixed seed power of $P_{seed} = 50\,mW$. Left: Variation of the RW current at a fixed TP current of $I_{TP} = 4\,A$. Right: Variation of the TP current at a fixed RW current of $I_{RW} = 600\,mA$.

the reflection geometry with the lens L5 and the mirror M1 yields the highest coupling efficiency of the feedback back into the TPA. Thus, the backwards propagating feedback inside the TPA is almost entirely coupled to the RW section.

Since the intention of this survey is the characterization of the feedback from the TPA, which may be enhanced due to the external feedback, it is important that the seed laser source is not affected by the feedback. With the optical isolator and the beam splitter BS1 an effective isolation of the DBR-RWL of $-45\,dB$ is achieved. It has been shown in [8] that the used DBR-RWL is only affected by a power loss less than 10 % up to feedback levels of $-25\,dB$. Thus, optical feedback up to $+20\,dB$ from the TPA is acceptable for this setup.

V. Experimental Results

The presentation of the experimental results is divided into two parts: The results with the TPA in a solitary MOPA configuration and the results with the TPA in the extended setup under external optical feedback.

A. Solitary MOPA

First, the required seed power for a sufficient saturation of the TPA is determined. The output power is measured at a fixed RW and TP current of 600 mA and 4 A, respectively, while varying the seed power provided by the DBR-RWL. The results are shown in fig. 4. Up to 10 mW seed power the output power strongly increases. For even higher seed power levels only a moderate raise can be noticed. A default seed power of 50 mW is defined for the further measurements ensuring a sufficient saturation of the TPA. Next, the influence of the applied currents to the RW and TP section is considered. In fig. 5 the optical output power of the TPA at a fixed seed power of 50 mW but varying RW or TP current is given. While the RW current influences the output power moderately the TP current has a much larger impact. Optical output powers of nearly 4 W can be achieved. The default working point is set to $I_{RW} = 600\,mA$ and $I_{TP} = 4\,A$ as already used for the saturation characteristic and yielding almost 2 W output power.

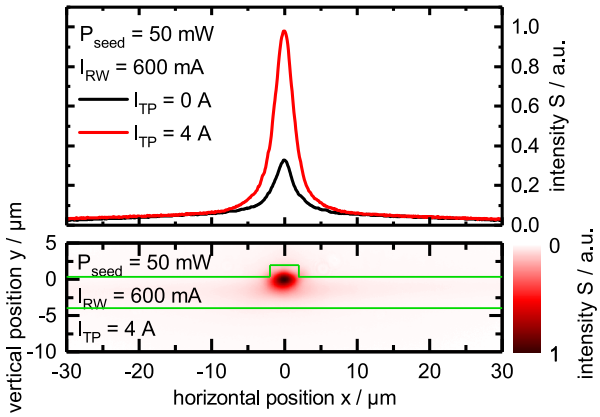

Fig. 6. Color map of the intensity distribution at back facet of the TPA (bottom). The TPA is seeded with $P_{seed} = 50\,mW$ and operated at RW and TP currents of $I_{RW} = 600\,mA$ and $I_{TP} = 4\,A$, respectively. The vertical slab waveguide and the center ridge waveguide are indicated in green. Vertically integrated intensity distribution at the same working point but with two different TP currents (top).

Before the amount of optical feedback emitted from the TPA is investigated, the spatial emission characteristics of the feedback at the back facet are studied. Fig. 6 shows the two-dimensional intensity distribution at the back facet of the TPA at the default working point, imaged by a camera as well as the vertically integrated intensity distributions at two different TP currents. For a better comparison the vertical waveguide and the ridge region are marked in green. Significant feedback light is only emitted from the center of the RW. A nearly Gaussian shaped intensity distribution is obtained with a weak homogeneous background. The background intensity distribution is better visible in the vertically integrated intensity profiles where no characteristic side lobes or higher order modes in the RW can be distinguished. In addition to the intensity profile at the default working point the intensity profile at $I_{TP} = 0\,A$ is shown. Although the output power of the TPA at this working point is nearly vanishing the background intensity stays at the

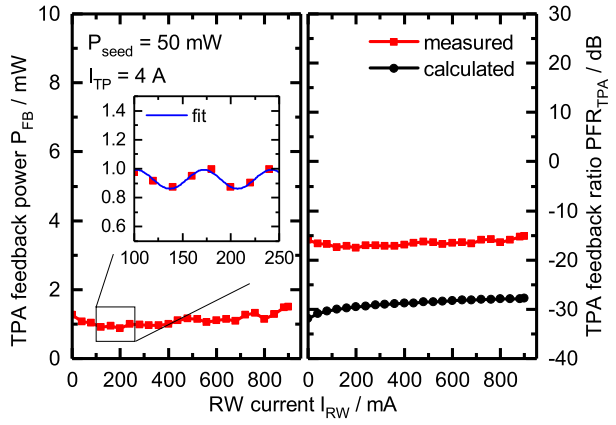

Fig. 7. Feedback power characteristics of the TPA at a fixed seed power of $P_{\text{seed}} = 50\,\text{mW}$ and TP current $I_{\text{TP}} = 4\,\text{A}$ as a function of RW current. Left: absolute value of the feedback power where the inset shows the indicated current range in more detail. Right: feedback power ratio in relation to the seed power.

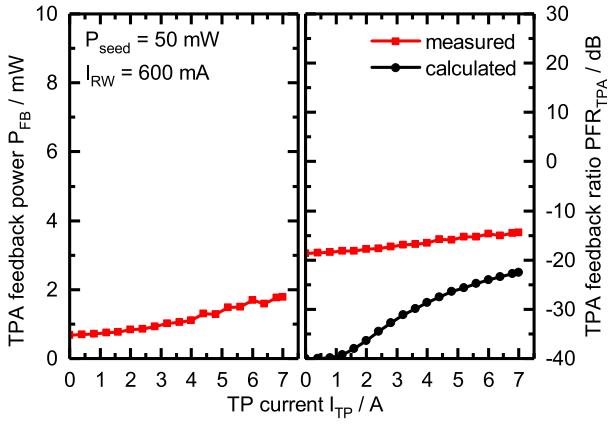

Fig. 8. Feedback power characteristics of the TPA at a fixed seed power of $P_{\text{seed}} = 50\,\text{mW}$ and RW current $I_{\text{RW}} = 600\,\text{mA}$ as a function of TP current. Left: absolute value of the feedback power. Right: feedback power ratio in relation to the seed power.

same level. Therefore, it can be concluded that the background intensity is mainly caused by ASE emission from the RW section. On the other hand, reflections at the front facet as well as ASE emission from the TP section do not contribute to the intensity distribution outside the RW, while light coupled into the RW increases the intensity of the central lobe significantly. While the TP current is raised from 0 A to 4 A the power content within the RW ($-2\,\mu\text{m} \leq x \leq 2\,\mu\text{m}$) nearly doubles from 21 % to 38 %.

In the following the dependency of the feedback power upon several operational parameters is presented. The influence of the RW current on the feedback power is depicted in fig. 7. On the left hand side the absolute feedback power is displayed. For a better overview and comparison with the feedback resistance of possible seed lasers, the results are also given as a feedback ratio in relation to the seed power of 50 mW on the right hand side. Additionally, the calculated feedback power ratio based on equation (6) and the measured optical output power (see fig. 5) is plotted. The feedback power is nearly constant around 1 mW or −15 dB with a small increase towards higher RW currents. Furthermore, the feedback power is characterized by tiny kinks and oscillations. Due to the non-vanishing reflectivity of the facets the TPA still forms a weak cavity. As the pump current affects the refractive index in the TPA and thereby the phase of the propagating light, resonance effects can be expected. To verify that the oscillations are related to a refractive index change in the RW section the periodicity of the oscillations is considered in detail. For a 2π phase change of the light reflected at the front facet the refractive index in the RW section changes by $\Delta n = \lambda/(2L_{\text{RW}}) = 2.8 \times 10^{-4}$ with the emission wavelength $\lambda = 1120\,\text{nm}$ of the MO. The dependency of the refractive index upon the injection current can be estimated from emission spectra measurements of a laser that features the same vertical and lateral design as the RW section of the TPA. A refractive index variation Δn causes a change of the emission wavelength λ by $\Delta\lambda = \lambda \Delta n / n_{\text{ref}}$ where n_{ref} is the reference refractive index. The spectral characterization of a DBR-RWL with 2 mm gain section length [18] yields that the emission wavelength changes with current I by $\Delta\lambda/\Delta I = 1.34\,\text{nm}\,\text{A}^{-1}$. With the reference refractive index $n_{\text{ref}} \approx 3.33$ [18] it can be calculated that a 2π phase change in the TPA occurs if the RW current is raised by approximately 70 mA. The inset of fig. 7 shows the TPA feedback power in more detail with more data points. The blue line displays a cosine function with 70 mA period length while the offset and amplitude are adapted to the measurement data. The calculated periodicity agrees with the measured data indicating a 2π phase change in the TPA.

The same raise of the feedback with the RW current is obtained with the calculation, however, the absolute feedback strength is underestimated by about one order of magnitude. The discrepancy between measurement and calculation can be traced back to the ASE emission from the TPA. This explanation is supported if the dependency of the feedback at varying TP current in fig. 8 is considered. While the output power (cf. fig. 5) ranges from almost 0 W to 4 W the feedback power stays between 0.7 mW and 1.9 mW. Especially at the TP current of 0 A with nearly zero output power feedback due to reflection at the front facet can be neglected compared to the reflection at the back facet with reflectivity 1×10^{-4}. The calculated curves therefore approach −40 dB at $I_{\text{TP}} = 0\,\text{A}$ whereas the measurement still yields feedback levels two orders of magnitude higher. That being so, the feedback emission due to ASE is much stronger than that originating from reflections at the facets.

Finally, the influence of the seed power on the feedback from the TPA in solitary MOPA configuration is covered. Fig. 9 shows the feedback from the TPA at the default working point but varying seed power. Complementary to the output power presented for the saturation characteristics of the TPA (fig. 4), the feedback power first strongly decreases with higher seed power, followed by an only small reduction for seed power levels greater than 10 mW. It is important to note that the feedback ratio presented on the right of fig. 9 is in relation to the actual seed power. Thus, even if the feedback power stays constant for further increase of the seed power

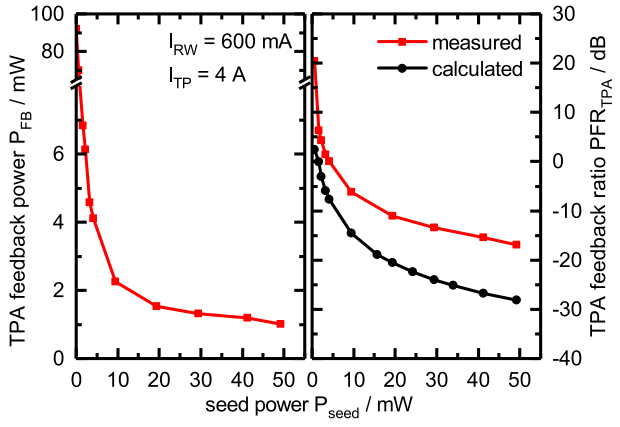

Fig. 9. Feedback power characteristics of the TPA at fixed RW and TP current of $I_{RW} = 600\,\text{mA}$ and $I_{TP} = 4\,\text{A}$ as a function of the seed power. Left: absolute value of the feedback power. Right: feedback power ratio in relation to the seed power.

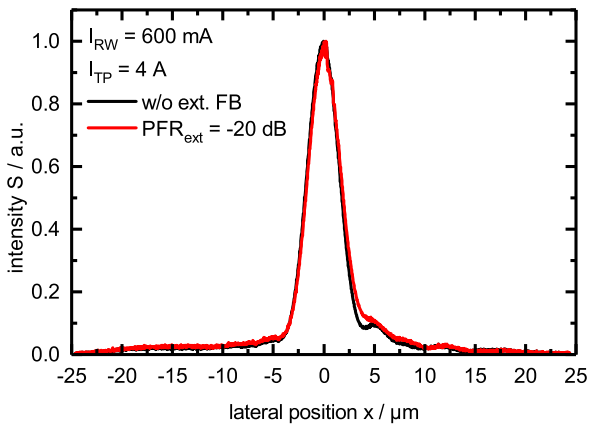

Fig. 11. Lateral beam waist intensity profile of the TPA output at a fixed seed power $P_{seed} = 50\,\text{mW}$ and RW and TP current of $I_{RW} = 600\,\text{mA}$ and $I_{TP} = 4\,\text{A}$ without external feedback in comparison with $PFR_{ext} = -20\,\text{dB}$ applied to the TPA.

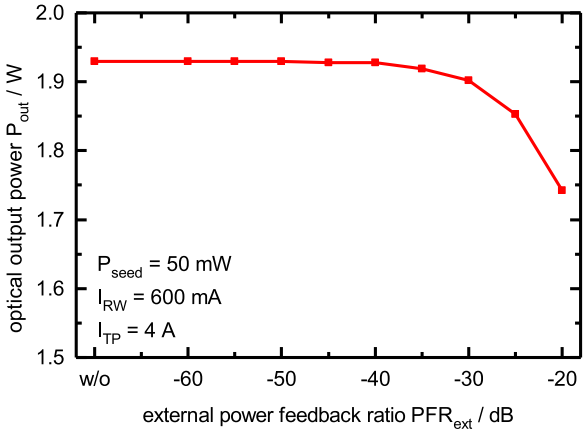

Fig. 10. Output power characteristics of the TPA at fixed seed power $P_{seed} = 50\,\text{mW}$ and RW and TP current of $I_{RW} = 600\,\text{mA}$ and $I_{TP} = 4\,\text{A}$ as a function of the external feedback applied to the TPA.

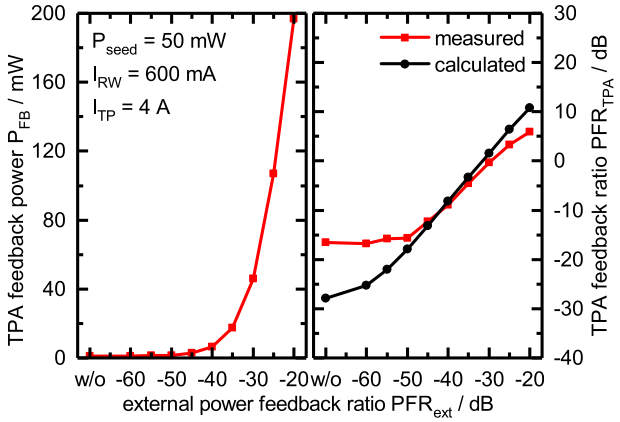

Fig. 12. Feedback power characteristics of the TPA at fixed seed power $P_{seed} = 50\,\text{mW}$ and RW and TP current of $I_{RW} = 600\,\text{mA}$ and $I_{TP} = 4\,\text{A}$ as a function of the external feedback applied to the TPA. Left: absolute value of the feedback power. Right: feedback power ratio in relation to the seed power.

the relative power ratio still decreases. From 10 mW to 50 mW seed power the power feedback ratio can be attenuated by one order of magnitude.

B. MOPA With External Feedback

Initially, the optical output power of the MOPA system is investigated under the influence of external optical feedback. The results are given in fig. 10. The output power decreases with raising external feedback slightly to 1.74 W with a significant change obtained for feedback strengths higher than −30 dB. In order to characterize the effect of the optical feedback on the spatial beam quality, the beam waist of the output beam is imaged onto a camera. In fig. 11 the lateral (x-direction) beam waist intensity profile is exemplary shown for the solitary MOPA (without feedback) and the maximum feedback strength of −20 dB. The beam waist intensity profile features a distinct Gaussian shaped central lobe with small side lobes. With −20 dB external feedback the side lobe intensity increases slightly indicating a degradation of beam quality. However, the influence of optical feedback on the spatial beam quality is small, while the beam waist profile remains unchanged for feedback ratios below −20 dB.

In contrast to the dependency of the output power upon external optical feedback the change of the feedback from the TPA is significantly more pronounced. In fig. 12 the feedback power of the TPA at the default working point is shown as a function of the external feedback strength. The feedback power stays nearly constant for external feedback levels up to −50 dB, whereas a strong increase of the feedback power follows for higher external feedback levels. At the highest external feedback level of −20 dB the feedback power from the TPA raises up to 200 mW, two orders of magnitude higher than in solitary MOPA operation. A comparison with the calculated feedback ratio yields a good agreement. Until −50 dB the feedback is dominated by the ASE emission but once the external feedback ratio is high enough the ASE emission becomes negligible with respect to the feedback resulting from

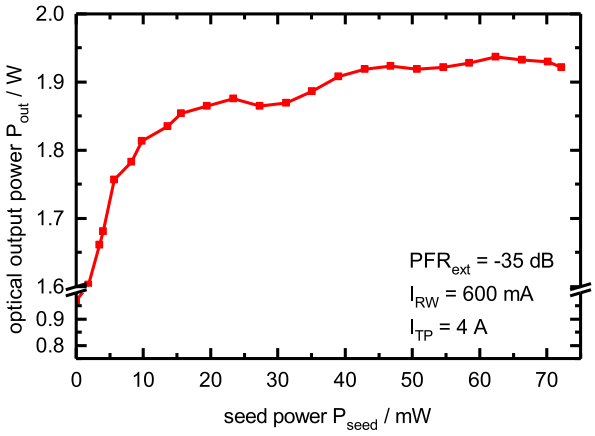

Fig. 13. Output power characteristics of the TPA at a fixed working point with $I_{\mathrm{RW}} = 600\,\mathrm{mA}$ RW current and $I_{\mathrm{TP}} = 4\,\mathrm{A}$ TP current and an external power feedback ratio of $-35\,\mathrm{dB}$ as a function of the input seed power.

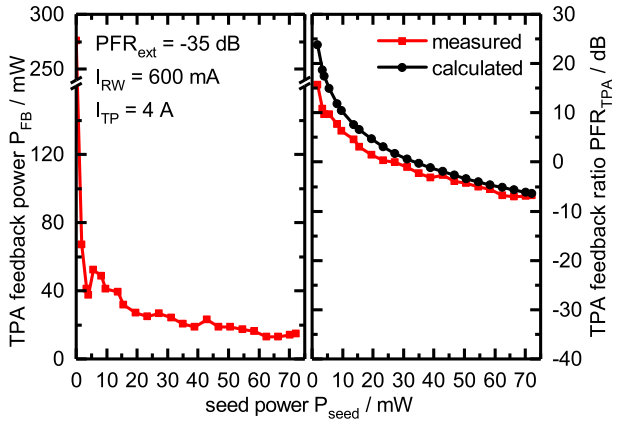

Fig. 14. Feedback power characteristics of the TPA at fixed external feedback ratio $PFR_{\mathrm{ext}} = -35\,\mathrm{dB}$ and RW and TP current of $I_{\mathrm{RW}} = 600\,\mathrm{mA}$ and $I_{\mathrm{TP}} = 4\,\mathrm{A}$ as a function of the seed power. Left: absolute value of the feedback power. Right: feedback power ratio in relation to the seed power.

the reflections. Consequently, the power content in the RW of the corresponding back facet intensity distribution increases significantly, since the external feedback is solely guided in the RW towards the back facet. At the maximum external feedback strength of $-20\,\mathrm{dB}$ the power content in the RW raises up to 62 %.

Finally, the effect of varying seed power on the TPA emission characteristics under external optical feedback is covered. As the default external feedback strength $-35\,\mathrm{dB}$ is chosen, which is a typical value for real life applications. The optical output power of the MOPA at this working point as a function of the seed power is given in fig. 13. The saturation characteristic is comparable to the characteristics in solitary MOPA operation presented in fig. 4. However, the output power shows a slight oscillation and the power drop at the lowest seed power in the unsaturated regime is less pronounced. Fig. 14 shows the dependency of the feedback emission from the TPA upon the seed power. Again, the feedback power is complementary to the output power with strongly increasing feedback at low seed power levels. By increasing the seed power above the working point of 50 mW the feedback power is still reduced but only by less than 30 %. An oscillating behavior is also observed, with local maximums of the feedback power matching the minimums of the output power and vice versa. Both, the beam waist of the MOPA output beam and the intensity distribution at the back facet of the TPA remain unchanged during the oscillatory behavior.

Since the feedback power is now dominated by reflected laser light the model describes the power feedback ratio much more accurately. Only at the lowest seed power the feedback is overestimated by the calculations.

The oscillations of the output and feedback power can be explained by resonance effects between the back facet and the external reflector. Since the external reflection is well coupled to the TPA the external reflectivity is much larger than the effective reflectivity of the front facet and is comparable to the reflectivity of the back facet. During the seed power variation the emission wavelength of the DBR-RWL changes, yielding different feedback phases.

In addition to the refractive index in the TPA the position of the external reflector M1 also affects the phase. A 2π phase change is obtained for a translation of M1 by $\lambda/2 = 560\,\mathrm{nm}$. To examine the effect of phase changes on the TPA feedback emission, the position of the mirror M1 is varied slightly, without modifying the coupling of the feedback significantly. Although the mirror can not be moved with sub-μm steps and a possible oscillation is not resolved, it is found that the feedback power changes with the mirror position. Here, relative power changes of $\pm 10\,\%$ are observed. For a quantitative measurement of the contrast of the oscillations, experiments with higher spatial resolution are needed.

VI. Conclusion

The feedback emission characteristics of a TPA emitting at 1120 nm in a MOPA configuration have been investigated with respect to its operating currents, the seed power and external feedback. In solitary MOPA operation the feedback power is of the order of 1 mW. A large amount of the feedback is ASE emission, while the reflections at the front and back facet are at least one order of magnitude smaller. Operated at around 2 W output power the pump current applied to the RW or TP section has only a small effect on the feedback power and similarly small is the influence of the seed power in the well saturated regime. With external feedback applied to the TPA the feedback power can increase by more than two orders of magnitude at a maximum external feedback ratio of $-20\,\mathrm{dB}$.

A simple formula for the calculation of the feedback power has been derived based only on the seed power, the back and front facet reflectivity as well as the external reflectivity. The calculated feedback power is a good estimate if the feedback is dominated by reflections, which is especially the case for external feedback. But the calculation still yields the qualitative emission behavior and a lower estimate for the case that the major part of the feedback is ASE emission. Especially in the solitary MOPA operation or with weak external feedback

below −50 dB a more sophisticated model is required. Here 2D simulation of the optical field with a model for ASE like [15] could provide better quantitative agreement with the measurement results.

With respect to the feedback sensitivity of seed laser sources and the development of MOPAs as a laser system for certain applications several conclusions can be made. First, the TPA should be operated in the well saturated regime. Although the output power of the TPA may raise only slowly for higher seed power levels the reduction of the relative power feedback ratio, which is the key influencing factor for the laser's feedback sensitivity, can be worth it. Second, even in the highly saturated regime the power feedback ratio is of the order of −15 dB requiring either a laser with extreme resistance against feedback [8], [19] or an optical isolator. Third, the occurrence of external feedback sources when using the MOPA has to be considered in detail. External feedback up to −50 dB does not increase the feedback emission but external reflectivities of −35 dB can enhance the feedback from the TPA by one order of magnitude.

Concerning the results of this work MOPA based laser sources can be optimized to an even greater extent for specific applications with unwanted optical feedback.

ACKNOWLEDGMENT

The authors would like to thank Dr. H. Wenzel and Dr. G. Blume for helpful discussions and valuable support.

REFERENCES

[1] W. Telford *et al.*, "DPSS yellow-green 561-nm lasers for improved fluorochrome detection by flow cytometry," *Cytometry Part A*, vol. 68A, no. 1, pp. 36–44, 2005.

[2] K. Inagaki, K. Ohkoshi, S. Ohde, G. A. Deshpande, N. Ebihara, and A. Murakami, "Comparative efficacy of pure yellow (577-nm) and 810-nm subthreshold micropulse laser photocoagulation combined with yellow (561–577-nm) direct photocoagulation for diabetic macular edema," *Jpn. J. Ophthalmol.*, vol. 59, no. 1, pp. 21–28, 2015.

[3] A. K. Hansen *et al.*, "Efficient generation of 1.9 W yellow light by cascaded frequency doubling of a distributed Bragg reflector tapered diode," *Appl. Opt.*, vol. 55, no. 32, pp. 9270–9274, 2016.

[4] A. Sahm, N. Werner, J. Hofmann, D. Jedrzejczyk, D. Feise, and K. Paschke, "Miniaturized watt-level laser modules emitting in the yellow-green spectral range for biophotonic applications," *Proc. SPIE*, vol. 10902, Mar. 2019, Art. no. 109020C.

[5] R. Bege *et al.*, "Reduction of optical feedback originating from ferroelectric domains of periodically poled crystals," *IEEE J. Quantum Electron.*, vol. 53, no. 5, pp. 1–9, Oct. 2017.

[6] D. J. Bossert, J. R. Marciante, and M. W. Wright, "Feedback effects in tapered broad-area semiconductor lasers and amplifiers," *IEEE Photon. Technol. Lett.*, vol. 7, no. 5, pp. 470–472, May 1995.

[7] S. Delepine *et al.*, "How to launch 1 W into single-mode fiber from a single 1.48-μm flared resonator," *IEEE J. Sel. Topics Quantum Electron.*, vol. 7, no. 2, pp. 111–123, Mar. /Apr. 2001.

[8] N. Werner, J. Wegemund, D. Feise, K. Paschke, and G. Tränkle, "Emission behavior of distributed Bragg-reflector ridge waveguide lasers exposed to strong optical feedback," *Appl. Opt.*, vol. 59, no. 28, pp. 8653–8660, 2020.

[9] K. Paschke *et al.*, "High brightness, narrow bandwidth DBR diode lasers at 1120 nm," *IEEE Photon. Technol. Lett.*, vol. 25, no. 20, pp. 1951–1954, Oct. 15, 2013.

[10] S. Sujecki *et al.*, "Nonlinear properties of tapered laser cavities," *IEEE J. Sel. Topics Quantum Electron.*, vol. 9, no. 3, pp. 823–834, May 2003.

[11] M. A. Helal, S. N. Nyirenda-Kaunga, S. Bull, and E. C. Larkins, "Beam quality degradation processes in tapered lasers and DBR tapered lasers," in *Proc. IEEE High Power Diode Lasers Syst. Conf. (HPD)*, Oct. 2017, pp. 25–26.

[12] P. Albrodt *et al.*, "Low-index quantum-barrier single-pass tapered semiconductor optical amplifiers for efficient coherent beam combining," *Semicond. Sci. Technol.*, vol. 35, no. 6, Jun. 2020, Art. no. 065018.

[13] M. A. Helal, S. N. Nyirenda-Kaunga, S. Bull, and E. C. Larkins, "Impact of unintentional external feedback on the performance of high-power tapered lasers," in *Proc. IEEE High Power Diode Lasers Syst. Conf. (HPD)*, Oct. 2017, pp. 21–22.

[14] G. Talli, "Amplified spontaneous emission in semiconductor optical amplifiers: Modelling and experiments," *Opt. Commun.*, vol. 218, nos. 1–3, pp. 161–166, Mar. 2003.

[15] J. J. Lim *et al.*, "Design and simulation of next-generation high-power, high-brightness laser diodes," *IEEE J. Sel. Topics Quantum Electron.*, vol. 15, no. 3, pp. 993–1008, May 2009.

[16] H. Wenzel, "Basic aspects of high-power semiconductor laser simulation," *IEEE J. Sel. Topics Quantum Electron.*, vol. 19, no. 5, Sep./Oct. 2013, Art. no. 1502913.

[17] M. Christensen, C. Zink, M. T. Jamal, A. K. Hansen, O. B. Jensen, and B. Sumpf, "Measuring the sensitivity to optical feedback of single-frequency high-power laser diodes," *J. Opt. Soc. Amer. B, Opt. Phys.*, vol. 38, no. 3, p. 885, 2021.

[18] N. Werner, G. Blume, D. Feise, F. Bugge, K. Paschke, and G. Trankle, "Spectral mode hop characteristics of ridge waveguide lasers with distributed Bragg-reflector," *IEEE Photon. Technol. Lett.*, vol. 29, no. 24, pp. 2183–2186, Dec. 15, 2017.

[19] Y. Matsui, R. Schatz, D. Che, F. Khan, M. Kwakernaak, and T. Sudo, "Low-chirp isolator-free 65-GHz-bandwidth directly modulated lasers," *Nature Photon.*, vol. 15, no. 1, pp. 59–63, Jan. 2021.

Nils Werner was born in Salzgitter, Germany, in 1990. He received the master's degree in physics from the University of Potsdam, Germany, in 2016. He is currently pursuing the Ph.D. degree with the Ferdinand-Braun-Institut gGmbH, Leibniz-Institut für Höchstfrequenztechnik, Berlin. His research interests include the development of hybrid integrated laser systems with a focus on optical feedback aspects, optimization of diode laser systems in the near-infrared spectral range as well as second-harmonic generation.

Nina Thieß received the bachelor's degree in applied physics and medical engineering from Berliner Hochschule für Technik, Berlin, Germany, in 2019. She joined the Ferdinand-Braun-Institut gGmbH, Leibniz-Institut für Höchstfrequenztechnik, Berlin, in 2019, as a bachelor student, where she also worked as a Student Assistant until 2021. Her research interests include edge-emitting diode lasers and amplifiers in the wavelength range around 1120 nm as well as optical feedback effects.

Katrin Paschke received the Diploma degree in physics from the University of Potsdam, Potsdam, Germany, in 1996, and the Ph.D. degree in electrical engineering from Technische Universität Berlin, Berlin, Germany, for the realization of a high-brilliance α-DFB laser, in 2006. In 1997, she joined the Ferdinand-Braun-Institut gGmbH, Leibniz-Institut für Höchstfrequenztechnik, Berlin, and worked initially on noise and reliability of optoelectronical devices. Since 2007, she has been a Group Leader at the Ferdinand-Braun-Institut, where she is responsible for the research on hybrid diode laser systems. Currently, she is the Head of the Laser Modules Laboratory, Ferdinand-Braun-Institut. Her research interests include the development of high-brightness diode lasers and the fabrication of hybrid diode laser systems in the infrared spectral range and with frequency conversion for laser light sources in the visible spectral range.

Günther Tränkle (Member, IEEE) received the Ph.D. degree in physics from the University of Stuttgart, Stuttgart, Germany, in 1988. In 1996, he became the Head of the Ferdinand-Braun-Institut gGmbH, Leibniz-Institut für Höchstfrequenztechnik, Berlin, Germany. Since 2002, he has been a Full Professor with TU Berlin, Berlin, having a Chair on microwaves and optoelectronics. From 2013 to 2018, he was the acting Director of the Leibniz-Institute for Crystal Growth, Berlin. His research interests include novel electronic and optoelectronic devices, modules, and systems based on III/V compound semiconductors, and their applications from communications to life sciences.